

# Generation of continuous-wave THz radiation by use of quantum interference

E.A. Korsunsky and D.V. Kosachiov\*

*Institut für Experimentalphysik, Technische Universität Graz, A-8010*

*Graz, Austria*

August 8, 2018

We propose a scheme for generation of continuous-wave THz radiation. The scheme requires a medium where three discrete states in a  $\Lambda$  configuration can be selected, with the THz-frequency transition between the two lower metastable states. We consider the propagation of three-frequency continuous-wave electromagnetic (e.m.) radiation through a  $\Lambda$  medium. Under resonant excitation, the medium absorption can be strongly reduced due to quantum interference of transitions, while the nonlinear susceptibility is enhanced. This leads to very efficient energy transfer between the e.m. waves providing a possibility for THz generation. We demonstrate that the photon conversion efficiency is approaching unity in this technique.

OCIS codes: 190.2620, 190.4410, 270.1670, 020.1670

Generation of coherent terahertz electromagnetic radiation is a subject of much current research. This radiation might have interesting potential applications for electronics, chemical analysis of materials, local radars, tomography, environment monitoring<sup>1</sup>, and also for quantum optics applications and for frequency standards<sup>2,3</sup>. The THz range is in the gap between the radio-frequency and the visible ranges. Therefore, neither conventional electronic (microwave) methods nor the photonic ones can be directly applied to generate coherent THz radiation. Pulsed THz fields are produced since early seventies and success-

---

\*permanent adress: Tyumentransgas Co, 627720 Yugorsk, Russia

fully used in different applications. However, to the best of our knowledge, a reliable source of *continuous-wave* (c.w.) THz radiation is not available up to now.

Here we propose a c.w. generation scheme based on the effect of quantum interference in multilevel quantum systems (atoms, molecules, dopants in solids) induced by applied electromagnetic radiation. In an optically dense media, the interference may be destructive for linear susceptibility (absorption and refraction), so that an otherwise opaque medium becomes transparent. This process is termed electromagnetically induced transparency (EIT)<sup>4</sup>. The cancellation of absorption and refraction can also be explained as being due to the preparation of atoms in a coherent superposition ("dark" state) which is immune to applied radiation. When all the atomic population is perfectly trapped in this superposition, the medium does not "see" the radiation. It turns out, however, that if the dark state is slightly disturbed the linear susceptibility remains still very small, while the nonlinear susceptibility is resonantly enhanced by constructive interference<sup>5</sup>. Therefore, nonlinear frequency conversion/generation processes are very efficient in such media. Several successful experiments have been performed demonstrating efficient generation of XUV radiation with atomic hydrogen<sup>6</sup>, red to blue frequency conversion with molecular sodium<sup>7</sup>, enhanced four-wave mixing with doped crystals<sup>8</sup>. Harris with coworkers have reached blue to UV<sup>9</sup> and UV to VUV<sup>10</sup> conversion in atomic Pb vapor with almost unity photon-conversion efficiency. The aim of the present paper is to extend these ideas to the case of THz generation, treating an interaction of the e.m. radiation with atoms as well as the propagation of radiation through the medium in exact manner.

We suggest that the THz radiation can be produced by the EIT-assisted frequency conversion in media where three discrete states may be selected, two of them being metastable ones. An example of such a scheme is a closed three-level  $\Lambda$  system (Fig. 1), where  $|1\rangle - |3\rangle$  and  $|2\rangle - |3\rangle$  are the dipole-allowed optical transitions, and the frequency of a magnetic-dipole transition  $|1\rangle - |2\rangle$  is in the THz range. Such systems can be found in vapors of alkaline-earth atoms with the corresponding states  $|1\rangle \equiv {}^3P_0$  or  ${}^3P_2$ ,  $|2\rangle \equiv {}^3P_1$  and  $|3\rangle \equiv {}^3S_1$ . Frequencies of the transitions  ${}^3P_0 - {}^3P_1$  and  ${}^3P_2 - {}^3P_1$  are 0.6 and 1.2 THz for  ${}^{24}\text{Mg}$ , 1.5 and 3.2 THz

for  $^{40}\text{Ca}$ , etc. A similar  $\Lambda$  system can be excited, for instance, in samarium atoms where the transition between two substates  $4f^6 6s^2 {}^7F_0$  and  ${}^7F_1$  of the ground state fine structure has a frequency of 8.78 THz. One may also find appropriate schemes in other atoms, where the THz transition is usually between the two fine structure components, and probably in some molecules and doped crystals as well.

Let us assume that the  $\Lambda$  atom interacts with a bichromatic optical field

$$\mathbf{E}(z, t) = \sum_{m=1,2} \mathbf{e}_{3m} E_{3m}(z, t) \frac{1}{2} \exp[-i(\omega_{3m}t - k_{3m}z + \varphi_{3m}(z, t))] + c.c. \quad (1)$$

having the frequencies  $\omega_{3m}$  resonant or near-resonant with transitions  $|m\rangle - |3\rangle$ ,  $m = 1, 2$ , and with the radiation of THz frequency  $\omega_T$

$$\mathbf{H}(z, t) = \mathbf{e}_T H(z, t) \frac{1}{2} \exp[-i(\omega_T t - k_T z + \varphi_T(z, t))] + c.c., \quad (2)$$

resonant with transition  $|1\rangle - |2\rangle$ . Here,  $E_{3m}$  and  $H$  are the amplitudes,  $\mathbf{e}_{3m}$  and  $\mathbf{e}_T$  are the unit polarization vectors,  $\varphi_{3m}$  and  $\varphi_T$  are the phases, and  $k_{3m} = \omega_{3m}/c$  and  $k_T = \omega_T/c$  are the wavenumbers of electric and magnetic field, respectively. Both the amplitudes  $E_{3m}$ ,  $H$  and the phases  $\varphi_{3m}$ ,  $\varphi_T$  are regarded as slowly varying functions of time and coordinate.

The propagation of e.m. waves along the  $z$  axis in the medium is governed by the Maxwell equations. In the slowly varying amplitude and phase approximation, these equations can be transformed to the following form<sup>11–13</sup>:

$$\frac{\partial E_{3m}}{\partial z} + \frac{1}{c} \frac{\partial E_{3m}}{\partial t} = -N \frac{4\pi d_{3m} \omega_{3m}}{c} \text{Im}(\tilde{\sigma}_{3m}), \quad (3a)$$

$$\frac{\partial \varphi_{3m}}{\partial z} + \frac{1}{c} \frac{\partial \varphi_{3m}}{\partial t} = -N \frac{4\pi d_{3m} \omega_{3m}}{c} \frac{1}{E_{3m}} \text{Re}(\tilde{\sigma}_{3m}), \quad (3b)$$

$$\frac{\partial H}{\partial z} + \frac{1}{c} \frac{\partial H}{\partial t} = -N \frac{4\pi \mu \omega_T}{c} \text{Im}(\tilde{\sigma}_{21}), \quad (3c)$$

$$\frac{\partial \varphi_T}{\partial z} + \frac{1}{c} \frac{\partial \varphi_T}{\partial t} = -N \frac{4\pi \mu \omega_T}{c} \frac{1}{H} \text{Re}(\tilde{\sigma}_{21}), \quad (3d)$$

where  $d_{3m} \equiv |\mathbf{e}_{3m} \mathbf{d}_{3m}|$ ,  $\mu \equiv |\mathbf{e}_T \vec{\mu}|$ ,  $\mathbf{d}_{3m}$  and  $\vec{\mu}$  are the matrix elements of the electric-dipole moment operator  $\hat{\mathbf{d}}$  and the magnetic-dipole moment operator  $\hat{\mu}$ , respectively, in the basis of bare atomic states  $|n\rangle$ ,  $n = 1, 2, 3$ :  $\mathbf{d}_{3m} \equiv \langle 3 | \hat{\mathbf{d}} | m \rangle$ ,  $\vec{\mu} \equiv \langle 1 | \hat{\mu} | 2 \rangle$ ;  $N$  is the density of the

active atoms. The medium polarization components (the right-hand side of Eqs. (3)) are determined by the density matrix elements  $\sigma_{ns}$  averaged over the atomic velocities with the distribution  $w(v_z)$  where  $v_z$  is the  $z$ -projection of the atom velocity:

$$\tilde{\sigma}_{ns} = \int_{-\infty}^{+\infty} dv_z w(v_z) \sigma_{ns}, \quad (4)$$

with

$$\sigma_{ns} = \rho_{ns}(v_z) \exp[i(\omega_{ns}t - k_{ns}z + \chi_{ns})], \quad (5)$$

where  $\rho_{ns} \equiv \langle n | \hat{\rho} | s \rangle$ ,  $\hat{\rho}$  is the atomic density matrix; and the phase  $\chi_{ns}$  is the sum of the e.m. field phase  $\varphi_{ns}$  and the phase  $\vartheta_{ns}$  of the atomic dipole moment  $\mathbf{d}_{3m} = |\mathbf{d}_{3m}| e^{i\vartheta_{3m}}$ ,  $\vec{\mu} = |\vec{\mu}| e^{i\vartheta_{12}}$ :  $\chi_{3m} = \varphi_{3m} + \vartheta_{3m}$ ,  $\chi_{12} = \varphi_T + \vartheta_{12}$ .

The  $\Lambda$  system represents a typical interaction scheme where the interference of excitation channels may lead to creation of a dark state and preparation of atoms in this state<sup>14</sup>. If the e.m. field between the states  $|1\rangle$  and  $|2\rangle$  is not applied then the following superposition of the metastable states

$$|NC\rangle = \frac{g_{32}/g_{31}}{\sqrt{1 + g_{32}^2/g_{31}^2}} |1\rangle - \exp(\chi_{32} - \chi_{31}) \frac{1}{\sqrt{1 + g_{32}^2/g_{31}^2}} |2\rangle, \quad (6)$$

gets completely decoupled from the field when the two-photon resonance condition is satisfied:

$$\Delta_{32} - \Delta_{31} = 0. \quad (7)$$

In Eqs. (6) and (7),  $g_{3m} = d_{3m}E_{3m}/2\hbar$  are the Rabi frequencies of the optical fields,  $\Delta_{3m} = \omega_{3m} - (\mathcal{E}_3 - \mathcal{E}_m)/\hbar$  are the laser frequency detunings from transitions  $|m\rangle - |3\rangle$ , ( $m = 1, 2$ ),  $\mathcal{E}_n$  is the eigenenergy of the atomic state  $|n\rangle$ . The superposition  $|NC\rangle$  is stable, and it is fed by spontaneous emission from the level  $|3\rangle$  so that all the atomic population is trapped in  $|NC\rangle$  after some optical pumping time. Therefore, the light ceases to interact with atoms and propagates through the medium without absorption and refraction. We note that this occurs for any relation between the laser intensities and phases.

At the same time, the preparation of atoms in the superposition of metastable states  $|1\rangle$  and  $|2\rangle$  means that the coherence  $\sigma_{12}$  is induced. Corresponding to the Eqs. (3 c,d), this should lead to a generation of the field with frequency  $(\omega_{31} - \omega_{32})$ . Such an EIT-assisted generation of a microwave radiation has recently been observed in atomic Cs vapor<sup>15</sup>. In general, the presence of a third e.m. field destroys the dark state, so that the optical waves start to interact with the medium. However, the degree of the destruction is very small if the generated field is weak. In the present case, the THz generation corresponds to the difference-frequency generation scheme<sup>16</sup>. If we suppose the photon conversion efficiency to be unity, that is for each photon of frequency  $\omega_{31}$  one THz-photon (and one photon of frequency  $\omega_{32}$ ) is generated, then the maximum energy (or power) conversion efficiency is given by  $\eta = \hbar\omega_T/\hbar\omega_{31} \ll 1$ . For example, for the  $\Lambda$  system ( $3^3P_1 - 3^3P_2 - 4^3S_1$ ) in  $^{24}\text{Mg}$ , we have  $\omega_T = 1.22 \cdot 10^{12}$  Hz,  $\omega_{31} = 5.80 \cdot 10^{14}$  Hz, and  $\eta = 0.0021$ . Therefore, the THz intensity is always much smaller than the optical one, so that the dark state disturbance is always very small. Thus, the total e.m. energy dissipation in the medium is negligible, and one can hope to get a very efficient generation in such a nearly dark ("grey") medium.

In this paper we concentrate on a regime of the radiation propagation in a continuous wave limit, that is, we shall assume that the characteristic time of a change in the field amplitudes and phases, and the interaction time of atoms with the radiation are much longer than the characteristic time of a change in the internal state of an atom. Then, the time derivatives in Eqs. (3) can be dropped, and the steady-state values of the density matrix elements  $\sigma_{ns}$  can be used in the right-hand side of Eqs. (3). The system considered here is an example of the so-called closed-loop system, where the steady state can be established only when the multi-photon resonance condition is satisfied<sup>17</sup>:

$$\omega_{31} - \omega_{32} - \omega_T = 0. \quad (8)$$

In what follows we will always assume the condition (8) to be fulfilled.

The density matrix equations for the  $\Lambda$  atom can be found in Refs.<sup>12,17</sup>. These equations can be solved analytically under some simplifying conditions. We suppose that spontaneous

relaxation rates for the channels  $|3\rangle \rightarrow |1\rangle$  and  $|3\rangle \rightarrow |2\rangle$  are equal:  $\gamma_{31} = \gamma_{32} \equiv \gamma$ . With the condition  $\omega_{31} \approx \omega_{32}$  (since  $(\omega_{31} - \omega_{32})/\omega_{31} = \omega_T/\omega_{31} \ll 1$ ) this would also imply  $|\mathbf{d}_{31}| \approx |\mathbf{d}_{32}|$ . This simplification allows us to get analytical results which demonstrate all the basic features of the process. Numerical calculations with real atomic parameters (Figs. 2-4) confirm the analytical results not only qualitatively, but even quantitatively. This suggests that the performance of the proposed scheme is not very sensitive to exact values of the relaxation rates and dipole moments on optical transitions. Another assumption used is quite reasonable. Since the THz radiation intensity is very small, we assume that its Rabi frequency is small:  $g_T = \mu H/2\hbar \ll \gamma$ .

Solution of the steady-state density matrix equations for  $v_z = 0$ ,  $\Gamma = 0$  ( $\Gamma$  is the relaxation rate of the coherence between states  $|1\rangle$  and  $|2\rangle$ ), equal spontaneous relaxation rates:  $\gamma_{31} = \gamma_{32} \equiv \gamma$ , and zero detunings  $\Delta_{31} = \Delta_{32} = 0$ , gives to the first order in  $(g_T/\gamma)$ :

$$\text{Im}(\sigma_{31}) = \frac{g_T g_{32}}{g_0^2} \sin \Phi, \quad (9a)$$

$$\text{Im}(\sigma_{32}) = -\frac{g_T g_{31}}{g_0^2} \sin \Phi, \quad (9b)$$

$$\text{Im}(\sigma_{21}) = -\frac{g_{31} g_{32}}{g_0^2} \sin \Phi, \quad (9c)$$

$$\text{Re}(\sigma_{31}) = -\frac{g_T g_{32} (g_{32}^2 - g_{31}^2)}{g_0^4} \cos \Phi, \quad (10a)$$

$$\text{Re}(\sigma_{32}) = \frac{g_T g_{31} (g_{32}^2 - g_{31}^2)}{g_0^4} \cos \Phi, \quad (10b)$$

$$\text{Re}(\sigma_{21}) = -\frac{g_{31} g_{32}}{g_0^2} \cos \Phi, \quad (10c)$$

The populations of the metastable states are

$$\begin{aligned} \rho_{11} &= \frac{g_{32}^2}{g_0^2} - \frac{2g_T g_{31} g_{32} \gamma}{g_0^4} \sin \Phi, \\ \rho_{22} &= \frac{g_{31}^2}{g_0^2} + \frac{2g_T g_{31} g_{32} \gamma}{g_0^4} \sin \Phi, \end{aligned}$$

where  $g_0^2 = g_{31}^2 + g_{32}^2$ , and the relative phase  $\Phi$  is determined as

$$\Phi = (\chi_{31} - \chi_{32}) - \chi_{12}. \quad (11)$$

The excited state population  $\rho_{33}$ , which is responsible for irreversible dissipation of the e.m. energy by the medium, is of the second order in  $(g_T / \gamma)$ . This indicates that atoms are really in the grey state. One sees from Eqs. (9) and (10), that the medium is absolutely transparent and not refractive for

$$\Phi = \pi n, \quad n = 0, 1, 2, \dots \quad (12)$$

and

$$g_{31} = g_{32}. \quad (13)$$

These are exactly the conditions for the dark state in closed  $\Lambda$  system<sup>12,17–19</sup>.

For arbitrary optical field amplitudes and phases, however, the refraction and absorption (or amplification) of individual frequency components may be substantial. The change of the fields can be calculated analytically by the method developed in paper by Armstrong *et. al.*<sup>20</sup>. We insert the density matrix elements (9) and (10) in the Maxwell equations (3).

The amplitude equations are read then:

$$\frac{dE_{31}}{dz} = -\frac{\pi N}{\hbar^2 c} \frac{d_{31}d_{32}\mu}{g_0^2} \omega_{31} E_{32} H \sin \Phi, \quad (14a)$$

$$\frac{dE_{32}}{dz} = \frac{\pi N}{\hbar^2 c} \frac{d_{31}d_{32}\mu}{g_0^2} \omega_{32} E_{31} H \sin \Phi, \quad (14b)$$

$$\frac{dH}{dz} = \frac{\pi N}{\hbar^2 c} \frac{d_{31}d_{32}\mu}{g_0^2} \omega_T E_{31} E_{32} \sin \Phi. \quad (14c)$$

The intensities associated with each of these waves are given by  $I_{3m} = (c/8\pi) E_{3m}^2$  and  $I_T = (c/8\pi) H^2$ . The set of equations (14) shows that the total power flow (proportional to the total intensity  $I = I_{31} + I_{32} + I_T$ ) is conserved, as expected for propagation through a lossless (due to EIT) medium:

$$\frac{dI}{dz} = \frac{dI_{31}}{dz} + \frac{dI_{32}}{dz} + \frac{dI_T}{dz} = \frac{N}{4\hbar^2} \frac{d_{31}d_{32}\mu}{g_0^2} (\omega_{32} + \omega_T - \omega_{31}) E_{31} E_{32} H \sin \Phi = 0,$$

where the last equality follows from the multiphoton resonance condition (8). Obviously, the energy losses (proportional to the population of the excited state  $\rho_{33}$ ) appear only in the second order in  $(g_T / \gamma)$ .

The set of equations (14) also implies that

$$\frac{d}{dz} \left( \frac{I_{31}}{\hbar\omega_{31}} \right) = -\frac{d}{dz} \left( \frac{I_{32}}{\hbar\omega_{32}} \right) = -\frac{d}{dz} \left( \frac{I_T}{\hbar\omega_T} \right), \quad (15)$$

which are the well-known Manley-Rowe relations<sup>16</sup>. These relations tell us that the rate at which photons at frequency  $\omega_T$  are created is equal to the rate at which photons at frequency  $\omega_{32}$  are created and is equal to the rate at which photons at frequency  $\omega_{32}$  are destroyed.

In order to solve the Maxwell equations, we introduce the following dimensionless variables: field amplitudes

$$u_m = \left( \frac{8\pi}{c} I \frac{\omega_{3m}}{\omega_0} \right)^{-1/2} E_{3m}, \quad (m = 1, 2),$$

$$u_T = \left( \frac{8\pi}{c} I \frac{\omega_T}{\omega_0} \right)^{-1/2} H,$$

where  $\omega_0 = (\omega_{31} + \omega_{32} + \omega_T)/2$ , and a dimensionless optical length  $\zeta = \kappa z$  with the coefficient

$$\kappa = \frac{4\pi N}{c} \frac{d_{31}d_{32}\mu}{g_0^2} \left( \frac{8\pi}{c} \frac{I}{\omega_0} \right)^{1/2} \sqrt{\omega_T\omega_{31}\omega_{32}}.$$

As we have discussed above, the THz intensity is always much smaller than the optical one:  $I_T \ll I_{31} + I_{32}$ . Therefore, we can safely assume that the total optical intensity  $I_{31} + I_{32} \approx I$  is conserved. This follows also from the first of the Manley-Rowe relations (15) taking into account the relation  $\omega_{31} \approx \omega_{32} \approx \omega_0$  (one can infer that an error in making such an approximation is of the order of  $\eta = (\omega_{31} - \omega_{32})/\omega_{31} = \omega_T/\omega_{31} \ll 1$ ). The conservation of the optical intensity may be written in variables  $u_m$  as follows:

$$u_1^2(\zeta) + u_2^2(\zeta) = 1. \quad (16)$$

Other "constants of motion" following from the Manley-Rowe relations (15) are:

$$u_1^2(\zeta) + u_T^2(\zeta) = B, \quad (17)$$

$$u_T^2(\zeta) - u_2^2(\zeta) = C, \quad (18)$$

where constants  $B$  and  $C$  are determined from the boundary conditions at the  $\zeta = 0$ .



Taking into account the assumed above closed values of the optical dipole moments:  $d_{31} \approx d_{32}$ , one concludes that the quantity  $g_0^2$  is also approximately constant over all the optical path, and it is approximately equal to  $(2\pi d_{31}^2/\hbar^2 c) I$ . All this allows one to write the amplitude and the phase Maxwell equations in variables  $u_m, \Phi$  as follows:

$$\frac{du_1}{d\zeta} = -u_2 u_T \sin \Phi, \quad (19a)$$

$$\frac{du_2}{d\zeta} = u_1 u_T \sin \Phi, \quad (19b)$$

$$\frac{du_T}{d\zeta} = u_1 u_2 \sin \Phi, \quad (19c)$$

$$\frac{d\Phi}{d\zeta} = \frac{u_T^2 (u_2^2 - u_1^2) - u_1^2 u_2^2}{u_1 u_2 u_T} \cos \Phi, \quad (19d)$$

where we have assumed that the atomic dipole phases  $\vartheta_{ns}$  do not change along the propagation path. The optical length can now be re-written as:

$$\zeta = \frac{\pi N}{\hbar^2 c} \mu \left( \frac{8\pi}{c} I \right)^{-1/2} \sqrt{\omega_T \omega_0} z. \quad (20)$$

The constants (16), (17) reduce the problem to solve of the set consisting of the first and the last of Eqs. (19). The right-hand side of Eq. (19 d) can be transformed to the following form by use of the first three Eqs. (19):

$$\frac{u_T^2 (u_2^2 - u_1^2) - u_1^2 u_2^2}{u_1 u_2 u_T} \cos \Phi = \frac{\cos \Phi}{\sin \Phi} \frac{1}{u_1 u_2 u_T} \frac{d(u_1 u_2 u_T)}{d\zeta}.$$

Therefore, the equation for the phase can be re-written as

$$\frac{d\Phi}{d\zeta} = \frac{\cos \Phi}{\sin \Phi} \frac{d}{d\zeta} (\ln(u_1 u_2 u_T)),$$

which can immediately be integrated to give the fourth constant of motion:

$$u_1 u_2 u_T \cos \Phi = \Pi. \quad (21)$$

The value of the constant  $\Pi$  can be determined from the known values of  $u_i$  and  $\Phi$  at the entrance to the medium,  $\zeta = 0$ . The expression (21) is used then to express  $\sin \Phi = \sqrt{1 - \cos^2 \Phi}$  in terms of the conserved quantity  $\Pi$ , and substitute it, together with the constants given in Eqs.(16), (17), into the Eq. (19 a). This gives:

$$\zeta = \pm \frac{1}{2} \int_{u_1^2(\zeta=0)}^{u_1^2} \frac{d(u_1^2)}{\sqrt{u_1^2(1-u_1^2)(B-u_1^2)-\Pi^2}}. \quad (22)$$

The integral in Eq. (22) can be reduced to the elliptic integral. In this paper we consider the case of the THz radiation generation. This situation corresponds to  $u_T(\zeta=0)=0$ ,  $B=u_{10}^2 \equiv u_1^2(\zeta=0)$ ,  $\Pi=0$ , and to the constant  $\cos \Phi$ :

$$\cos \Phi(\zeta) = 0. \quad (23)$$

Introduction of a quantity  $y = u_1/u_{10}$  leads to the elliptic integral of the first kind<sup>21</sup> in standard form:

$$\zeta = \pm \int_{y_0}^y \frac{dy}{\sqrt{(1-y^2)(1-u_{10}^2 y^2)}}.$$

The solution can be written then through sinus Jacobi elliptic functions:

$$u_1^2(\zeta) = u_{10}^2 sn^2[(\zeta + \zeta_0); u_{10}], \quad (24a)$$

$$u_2^2(\zeta) = 1 - u_{10}^2 sn^2[(\zeta + \zeta_0); u_{10}], \quad (24b)$$

$$u_T^2(\zeta) = u_{10}^2 \left(1 - sn^2[(\zeta + \zeta_0); u_{10}]\right). \quad (24c)$$

The solution indicates that as the optical length increases, energy is periodically transferred between the e.m. waves. The initial condition  $u_T(\zeta=0)=0$  requires that the constant  $\zeta_0$  is equal to  $\pm \mathbf{K}(u_{10})$ , the complete elliptic integral

$$\mathbf{K}(u_{10}) = \int_0^1 \frac{dy}{\sqrt{(1-y^2)(1-u_{10}^2 y^2)}},$$

which is a quarter-period of the function  $sn$ . Thus, the period of intensity oscillations is equal to  $2\mathbf{K}(u_{10})$  and the maximum possible power transferred to the THz radiation:  $u_T^2 = u_{10}^2$  occurs in a length

$$\zeta_{max} = \mathbf{K}(u_{10}). \quad (25)$$

The value of the function  $\mathbf{K}(u_{10})$  is close to  $\pi/2$  at  $u_{10} \ll 1$  and it is increased with  $u_{10}$  up to infinity at the limit  $u_{10} = 1$ <sup>21</sup>. For  $u_{20}^2 = 1 - u_{10}^2 \ll 1$  a half period can be approximated by

$$\mathbf{K}(u_{10}) = \frac{1}{2} \ln \left( \frac{16}{u_{20}^2} \right) \quad (26)$$

In terms of the real intensity, the Eq. (24 c) for the THz radiation can be written:

$$I_T(\zeta) = I_{31}(\zeta = 0) \frac{\omega_T}{\omega_{31}} \left( 1 - cd^2 [\zeta; u_{10}] \right). \quad (27)$$

We observe that at the length  $\zeta_{max} = \mathbf{K}(u_{10})$  the optical field is converted into the THz radiation with unity photon efficiency.

The obtained results are confirmed by numerical calculations of the Maxwell equations (3) with full density matrix calculations without any approximation. Figure 2 demonstrates the evolution of the e.m. wave intensities and the relative phase  $\Phi$  with the length for real parameters of the  $3^3P_1 - 3^3P_2 - 4^3S_1$  system in  $^{24}\text{Mg}$  atomic vapor. The optical length in this and all following figures is plotted in terms of a single-atom absorption cross-section for the optical field  $\tau = \left( 3\pi c^2 / 2\omega_{31}^2 \right) Nz$ , which has an advantage of being independent of total intensity  $I$ . The length  $\zeta$  introduced in Eq. (20) is connected to  $\tau$  by

$$\zeta = \tau \frac{\mu}{d_{31}} \sqrt{\frac{\omega_T}{\omega_{31}}} \left( \frac{\hbar \gamma_{31}}{d_{31}} \right) \left( \frac{8\pi}{c} I \right)^{-1/2}.$$

In order to compare the numerical and analytical calculations, the results presented in Fig. 2 are calculated for  $\Gamma = 0$ ,  $\Delta_{31} = \Delta_{32} = 0$ , and vapor temperature  $T = 10^{-3}K$  (i.e., in fact, for  $v_z = 0$ ). However, the atomic data (wavelengths, dipole moments and decay rates) are real. In particular, the spontaneous relaxation rates are not equal:  $\gamma_{32} = 1.66\gamma_{31}$ . The intensities at the entrance to the medium are chosen so that  $u_{20}^2 = 0.59 \cdot 10^{-4}$ . The dotted line in Fig. 2(b) is a calculation with formula (27) for  $u_{20}^2 = 0.55 \cdot 10^{-4}$ . One can see that the correspondence not only in the shape but also in quantitative characteristics of the process is excellent. The difference in parameter  $u_{20}^2$  is obviously due to the difference of spontaneous relaxation rates. As expected from analytical calculations, the transfer of energy to the THz radiation occurs with unity photon efficiency (the maximum value of  $I_T$  is exactly equal to  $0.0021I_{31}(\zeta = 0)$ ) at the length  $\tau_{max} = 7.6 \cdot 10^5$  ( $\zeta_{max} = 5.87$ , this value is quite close to that calculated from Eq. (26) for  $u_{20}^2 = 0.59 \cdot 10^{-4}$ :  $\zeta_{max} = 6.25$ ). Such a perfect

frequency conversion is due to the negligible decay of the dark state given by  $\Gamma$  and terms to the second order in  $g_T/\gamma$ . For the parameters of Fig. 2, the maximum THz intensity  $I_T = 0.0021I_{31}(\zeta = 0)$  corresponds to the Rabi frequency of only  $g_T \approx 8 \cdot 10^{-4} \gamma_{31}$ . The behavior of the phase  $\Phi$  in Fig. 2(c) also follows the law  $\cos \Phi(\zeta) = 0$  obtained analytically. The jumps in the phase occur at points where the intensity of the field being absorbed approaches zero, according to Eqs. (3 (b,d)).

In reality, however, we do have both the Doppler broadening and the relaxation rate  $\Gamma$  of the coherence between states  $|1\rangle$  and  $|2\rangle$ . Quantitatively, this considerably modifies the process. In Fig. 3 the spatial dependence of the field intensities and the phase  $\Phi$  are plotted for the vapor temperature  $T = 800\text{ K}$  (this gives the saturated vapor density of  $N = 1.7 \cdot 10^{15}\text{ cm}^{-3}$  and corresponds to the most probable velocity of atoms of  $v_p = 7.5 \cdot 10^4\text{ cm/sec}$ ),  $\Gamma = 10^{-4}\gamma_{31}$  (0.6 kHz), input Rabi frequencies  $g_{31}(\tau = 0) = 60\gamma_{31}$ ,  $g_{32}(\tau = 0) = 20\gamma_{31}$  (corresponding to laser intensities of  $I_{31} = 18.8\text{ W/cm}^2$  and  $I_{32} = 2.1\text{ W/cm}^2$ ). We see that the dynamics of the intensities and the phase does not change qualitatively as compared to the case of negligible decay of the dark state (Fig. 2). The THz radiation is generated and reaches its maximum,  $I_T = 39\text{ mW/cm}^2$  (Rabi frequency  $g_T \approx 4.6 \cdot 10^{-3} \gamma_{31}$ ) at the length  $\tau = 2.2 \cdot 10^6$  (for  $T = 800\text{ K}$  this corresponds to the real length of the gas cell of  $z = 4\text{ cm}$ ). A minor quantitative difference compared to the Fig. 2 case is that the optical length scale of the oscillations increases. This is simply a consequence of the optical length dependence on the total intensity, Eq. (20). However, the Doppler broadening, together with the rate  $\Gamma$ , considerably influence the efficiency of the frequency conversion. The efficiency reaches a maximum when the atoms are prepared in an almost dark state so that the energy dissipation is very weak. The dark state preparation relies in present case on the optical pumping. Therefore, the optical pumping rate should be much larger than the dark state decay in order to allow the population trapping in  $|NC\rangle$ . This requirement results in the following condition<sup>22</sup>:

$$\frac{g_0^2}{\gamma^2 + \Delta^2} \gg \frac{\Gamma}{\gamma},$$

where detuning  $\Delta$  includes the Doppler shift:  $\Delta = \Delta_{31} - k_{31}v_z \approx \Delta_{32} - k_{32}v_z$ . For the resonance  $\Delta_{31} = \Delta_{32} = 0$  and large Doppler broadening  $k_{31}v_p \gg \gamma$ , this condition reduces to

$$g_0^2 \gg \frac{\Gamma}{\gamma} (k_{31}v_p)^2 \quad (28)$$

or, in terms of intensity,

$$I \gg \frac{\Gamma}{\gamma} \left( \frac{k_{31}v_p}{\gamma} \right)^2 \frac{16\pi^2 \hbar \gamma c}{3\lambda_{31}^3}. \quad (29)$$

For the here considered case of  $^{24}\text{Mg}$  atoms at temperature  $800\text{K}$ , the total input intensity should be larger than  $3.75 \cdot 10^3 \cdot \Gamma/\gamma$  [ $\text{W}/\text{cm}^2$ ]. An importance of the condition (28) is demonstrated in Fig. 4. While the efficiency is approaching maximum:  $\eta = 2.06 \cdot 10^{-3}$ , for the parameters of Fig. 3 where  $\Gamma/\gamma = 10^{-4}$ , it drops to  $\eta = 1.66 \cdot 10^{-3}$  for  $\Gamma/\gamma = 2 \cdot 10^{-3}$  in Fig. 4 (a). Moreover, the intensity oscillations decay quite fast, and at the length  $\tau \geq 4 \cdot 10^6$  ( $\zeta \geq 4.87$ ) the optical fields are completely absorbed by the medium (not shown). Increase of the input intensity in Fig. 4 (b) leads to better trapping, weaker e.m. energy dissipation and, correspondingly, to larger conversion efficiency increasing to  $\eta = 2.00 \cdot 10^{-3}$ . Of course, with increasing input intensity the length scale of the conversion increases as well. Parameters of Fig. 4 (b) correspond to input intensities  $I_{31} = 470 \text{ W}/\text{cm}^2$  and  $I_{32} = 52 \text{ W}/\text{cm}^2$ , and to the maximum THz intensity of  $I_T = 0.94 \text{ W}/\text{cm}^2$  (Rabi frequency  $g_T \approx 2.3 \cdot 10^{-2} \gamma_{31}$ ) generated at  $\tau = 1.1 \cdot 10^7$  ( $z = 20 \text{ cm}$ ).

Thus, a practical realization of the proposed here generation scheme requires large optical length (large atom density), fairly large input intensities of the optical fields and small decay rate  $\Gamma$  of the atomic coherence  $\sigma_{12}$ . The rate  $\Gamma$  is determined by uncorrelated laser fluctuations, atomic collisions and other random phase disturbing processes. It has recently been experimentally demonstrated that, in a buffer gas, the coherence  $\sigma_{12}$  can survive a very large number of atomic collisions<sup>23,24</sup>. For instance, the rate  $\Gamma < 50 \text{ Hz}$  has been observed in experiment<sup>23</sup>. The correlation of the fluctuations in  $\omega_{31}$  and  $\omega_{32}$  radiations may be achieved if, for example, the  $\omega_{32}$  frequency is generated from  $\omega_{31}$  by operation of a Raman laser, as in Ref.<sup>7</sup>.

An important point in nonlinear frequency conversion is a phase matching. In our scheme, however, the optical frequencies are quite close in magnitude to each other. Therefore, the wave vectors  $k_{3m}$  change approximately equally due to dispersion of the medium, induced by the interaction with far-detuned states other than those of the  $\Lambda$  system. Thus, this phase mismatch may be neglected. Moreover, as it has been shown theoretically and experimentally<sup>9</sup>, the phase mismatch can be compensated for by very small value of two-photon detuning ( $\Delta_{31} - \Delta_{32}$ ), if it does appear.

In the particular case of Mg atoms, considered here as an illustrative example, the metastable states  $3^3P_1$  and  $3^3P_2$  are not the ground states. Therefore, one has to prepare an atomic ensemble in metastable states. This problem may be solved, for example, through a low-energy high-current electric discharge<sup>3</sup>. Another problem is that the state  $3^3P_1$  decays spontaneously to the ground state  $3^1S_0$ . However, the rate of this decay,  $4.3 \cdot 10^2 \text{ sec}^{-1} = 1.2 \cdot 10^{-5} \gamma_{31}$  is too slow to produce considerable effect on the process, presented here. Of course, all these problems may be avoided if one uses atoms with the metastable states  $|1\rangle$  and  $|2\rangle$  being the ground states, like in Sm atoms.

In conclusion, we have proposed a scheme for generation of continuous-wave THz radiation. Our scheme is based on a nonlinear interaction of three e.m. waves in atomic media with a  $\Lambda$  configuration of levels. An important ingredient of the scheme is a preparation of atoms in the grey state. As a consequence, the e.m. fields propagate through the medium with very weak dissipation of energy. Therefore the process may be considered as a parametric difference-frequency generation, where the THz frequency is the difference between two optical ones. We have obtained an analytical solution of the e.m. propagation problem which demonstrates that the intensities oscillate along the propagation path in a form of Jacobi elliptic functions. This allows us to predict that the photon conversion efficiency approaches unity in this technique, and to estimate the optical length at which the energy transfer from the optical field into the THz one is maximum. The analytical solution is confirmed by numerical calculations taking into account Doppler broadening and relaxation of the grey state. These calculations show that the efficiency of the THz generation remains

still very high in real situations, if the input optical intensity is sufficiently high to satisfy the condition (29). We note finally that the tuning of obtained THz radiation may be realized by shifting the metastable state energies via strong static magnetic or/and electric fields.

## 1. Acknowledgments

We are very grateful to Prof. L. Windholz for his continuous interest to this work and useful discussions. D.V. Kosachiov thanks the members of the Institut für Experimentalphysik, TU Graz, for hospitality and support. This study was supported by the Austrian Science Foundation under project No. P 12894-PHY.

E. Korsunsky's e-mail address is e.korsunsky@iep.tu-graz.ac.at.

- 
1. Special issue on "Terahertz electromagnetic pulse generation, physics, and applications", J. Opt. Soc. Amer. B **11**, No. 12, 2454-2581 (1994).
  2. F. Strumia, "A proposal for a new absolute frequency standard, using a Mg or Ca atomic beam", Metrologia **8**, 85-90 (1972).
  3. A. Godone and C. Novero, "The magnesium frequency standard", Metrologia **30**, 163-181 (1993).
  4. S.E. Harris, "Electromagnetically induced transparency", Physics Today **50**, No. 7, 36-42 (1997).
  5. S.E. Harris, J.E. Feld, and A. Imamoglu, "Nonlinear optical processes using electromagnetically induced transparency", Phys. Rev. Lett. **64**, 1107-1110 (1990).
  6. G.Z. Zhang, D.W. Tokaryk, B.P. Stoicheff, and K. Hakuta, "Nonlinear generation of extreme-ultraviolet radiation in atomic hydrogen using electromagnetically induced transparency", Phys. Rev. A **56**, 813-819 (1997); D.W. Tokaryk, G.Z. Zhang, and B.P. Stoicheff, "Nonlinear

- optical generation in a hydrogen discharge”, Phys. Rev. A **59**, 3116-3119 (1999).
7. S. Babin, U. Hinze, E. Tiemann, and B. Wellegehausen, ”Continuous resonant four-wave mixing in double- $\Lambda$  level configurations of  $\text{Na}_2$ ”, Opt. Lett. **21**, 1186-1188 (1996); A. Apolonskii, S. Balushev, U. Hinze, E. Tiemann, and B. Wellegehausen, ”Continuous frequency up-conversion in double- $\Lambda$  scheme of  $\text{Na}_2$ ”, Appl. Phys. B **64**, 435 (1997).
  8. B. S. Ham, M. S. Shahriar, and P. R. Hemmer, ”Enhanced nondegenerate four-wave mixing owing to electromagnetically induced transparency in a spectral hole-burning crystal”, Opt. Lett. **22**, 1138-1140 (1997); ”Enhancement of four-wave mixing and line narrowing by use of quantum coherence in an optically dense double- $\Lambda$  solid”, Opt. Lett. **24**, 86-88 (1999).
  9. M. Jain, H. Xia, G.Y. Yin, A.J. Merriam, and S.E. Harris, ”Efficient nonlinear frequency conversion with maximal atomic coherence”, Phys. Rev. Lett. **77**, 4326-4329 (1996).
  10. A.J. Merriam, S.J. Sharpe, H. Xia, D. Manuszak, G.Y. Yin, and S.E. Harris, ”Efficient gas-phase generation of coherent vacuum ultraviolet radiation”, Opt. Lett. **24**, 625-627 (1999).
  11. M.O. Scully and M.S. Zubairy, *Quantum Optics* (Cambridge University Press, Cambridge, 1997).
  12. D.V. Kosachiov, ”Resonant  $\Lambda$  medium as a converter of the laser radiation frequency”, Kvant. Elektron. **22**, 1123 (1995) [Quant. Electronics **25**, 1089 (1995)].
  13. E.A. Korsunsky and D.V. Kosachiov, ”Phase-dependent nonlinear optics with double- $\Lambda$  atoms”, Phys. Rev. A **60**, in press (1999).
  14. E. Arimondo, ”Coherent population trapping in laser spectroscopy”, in: *Progress in Optics* **35**, 257-354, ed. E. Wolf (Elsevier, Amsterdam, 1996).
  15. A. Godone, F. Levy, and J. Vanier, ”Coherent microwave emission in cesium under coherent population trapping”, Phys. Rev. A **59**, R12-R15 (1999); J. Vanier, A. Godone, and F. Levy, ”Coherent population trapping in cesium: dark lines and coherent microwave emission”, Phys.



- Rev. A **58**, 2345-2358 (1998).
16. R.W. Boyd, *Nonlinear Optics* (Academic Press, San Diego, 1992).
  17. D.V. Kosachiov, B.G. Matisov, and Yu.V. Rozhdestvensky, "Coherent phenomena in multi-level systems with closed interaction contour", J. Phys. B **25**, 2473-2488 (1992).
  18. S.J. Buckle, S.M. Barnett, P.L. Knight, M.A. Lauder, and D.T. Pegg, "Atomic interferometers: phase-dependence in multilevel atomic transitions", Opt. Acta **33**, 2473 (1986).
  19. D. Kosachiov, B. Matisov, and Yu. Rozhdestvensky, "Coherent population trapping: sensitivity of an atomic system to the relative phase of exciting fields", Opt. Commun. **85**, 209 (1991).
  20. J.A. Armstrong, N. Bloembergen, J. Ducuing, and P.S. Pershan, "Interactions between light waves in a nonlinear dielectric", Phys. Rev. **127**, 1918 (1962).
  21. *Handbook of Mathematical Functions*, ed. by M. Abramowitz and I.A. Stegun (Dover, New York, 1965).
  22. E.A. Korsunsky, W. Maichen, and L. Windholz, "Dynamics of coherent optical pumping in a sodium atomic beam", Phys. Rev. A **56**, 3908-3915 (1997).
  23. S. Brandt, A. Nagel, R. Wynands, and D. Meschede, "Buffer-gas-induced linewidth reduction of coherent dark resonances to below 50 Hz", Phys. Rev. A **56**, R1063-R1066 (1997).
  24. J.H. Xu and G. Alzetta, "High buffer gas pressure perturbation of coherent population trapping in sodium vapors", Phys. Lett. A **248**, 80-85 (1998).

## Figure captions

Fig. 1. Closed  $\Lambda$  system with two metastable states  $|1\rangle$  and  $|2\rangle$ .  $\omega_{31}$  and  $\omega_{32}$  are the optical frequencies,  $\omega_T$  is the THz-range frequency.

Fig. 2. Spatial variations of the optical (a) and THz (b) field intensities and the relative phase  $\Phi$  (c) in a vapor of  $^{24}\text{Mg}$  atoms interacting with radiation in a closed  $\Lambda$  configuration of levels  $3^3P_1 - 3^3P_2 - 4^3S_1$ . For this system, the relaxation rates are  $\gamma_{31} = 3.46 \cdot 10^7 \text{ sec}^{-1}$ ,  $\gamma_{32} = 1.66\gamma_{31}$ ,  $\gamma_{21} = 2.6 \cdot 10^{-14}\gamma_{31}$ , the wavelengths  $\lambda_{31} = 517.27 \text{ nm}$ ,  $\lambda_{32} = 518.36 \text{ nm}$ . Other parameters are: vapor temperature  $T = 10^{-3} \text{ K}$ ,  $\Gamma = 0$ , detunings  $\Delta_{31} = \Delta_{32} = 0$ , Rabi frequencies of input fields  $g_{31}(\tau = 0) = 10\gamma_{31}$ ,  $g_{32}(\tau = 0) = 0.1\gamma_{31}$  and  $g_{12}(\tau = 0) = 0$ . The dotted curve in (b) is a calculation with formula (27) for  $u_{20}^2 = 0.55 \cdot 10^{-4}$ .

Fig. 3. Spatial variations of the optical (a) and THz (b) field intensities and the relative phase  $\Phi$  (c) in a vapor of  $^{24}\text{Mg}$  atoms for vapor temperature  $T = 800 \text{ K}$ ,  $\Gamma = 10^{-4}\gamma_{31}$ , detunings  $\Delta_{31} = \Delta_{32} = 0$ , Rabi frequencies of input fields  $g_{31}(\tau = 0) = 60\gamma_{31}$ ,  $g_{32}(\tau = 0) = 20\gamma_{31}$  and  $g_{12}(\tau = 0) = 0$ . Other parameters are the same as in Fig. 2.

Fig. 4. Spatial variations of the THz radiation intensity in a vapor of  $^{24}\text{Mg}$  atoms for  $\Gamma = 2 \cdot 10^{-3}\gamma_{31}$  and Rabi frequencies of input fields: (a)  $g_{31}(\tau = 0) = 60\gamma_{31}$ ,  $g_{32}(\tau = 0) = 20\gamma_{31}$  and (b)  $g_{31}(\tau = 0) = 300\gamma_{31}$ ,  $g_{32}(\tau = 0) = 100\gamma_{31}$ . Other parameters are the same as in Fig. 3. Notice the different length scales in (a) and (b).

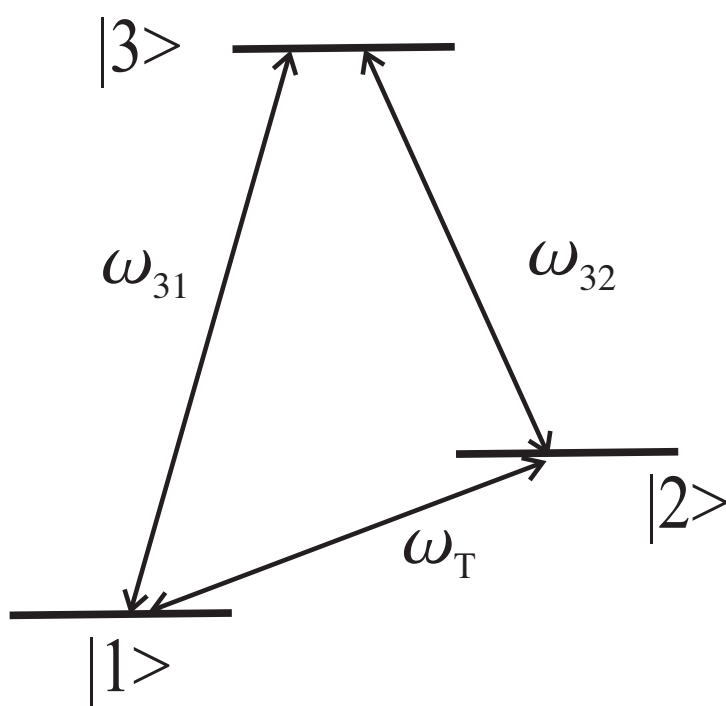


Fig. 1

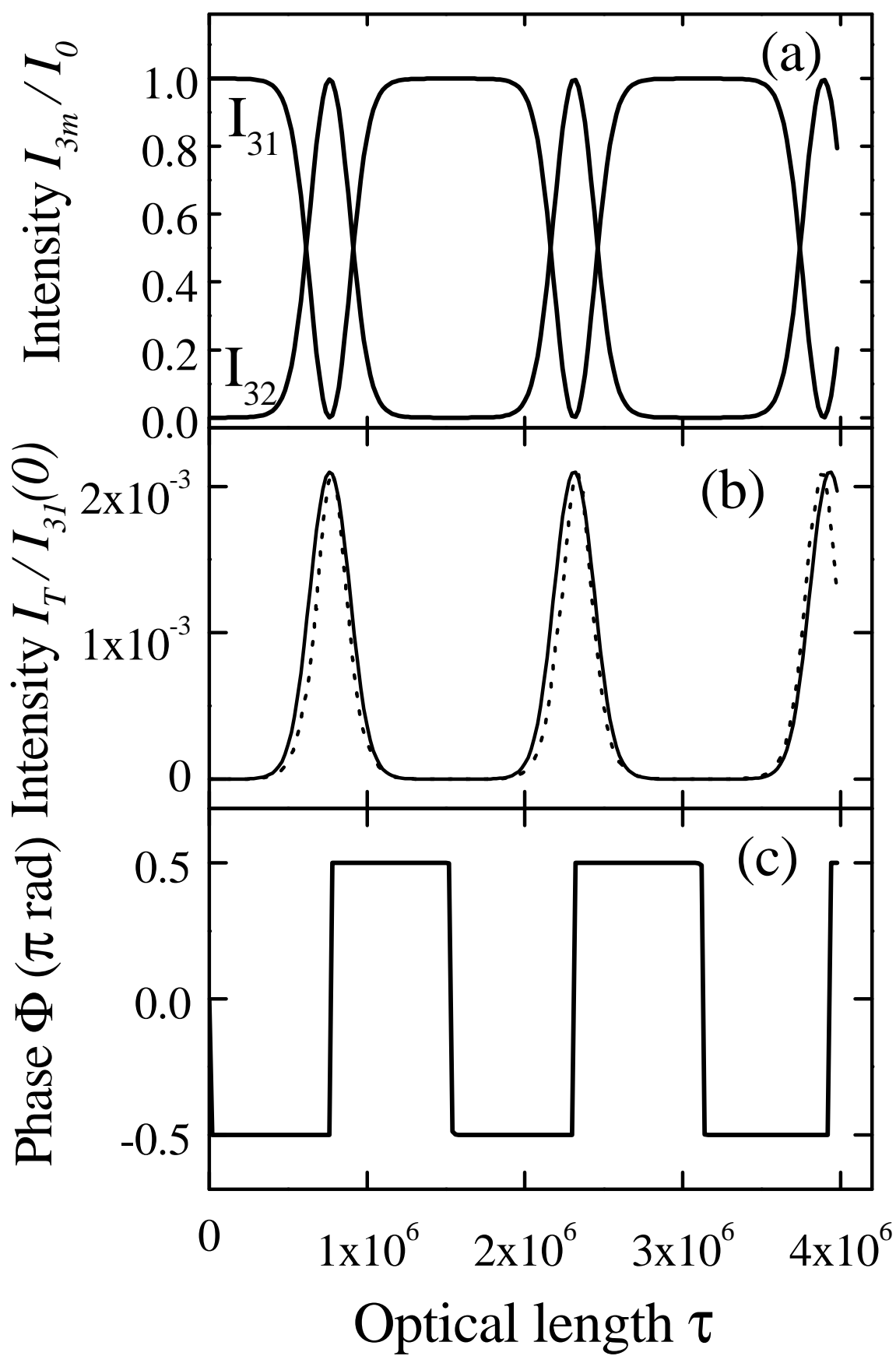


Fig. 2

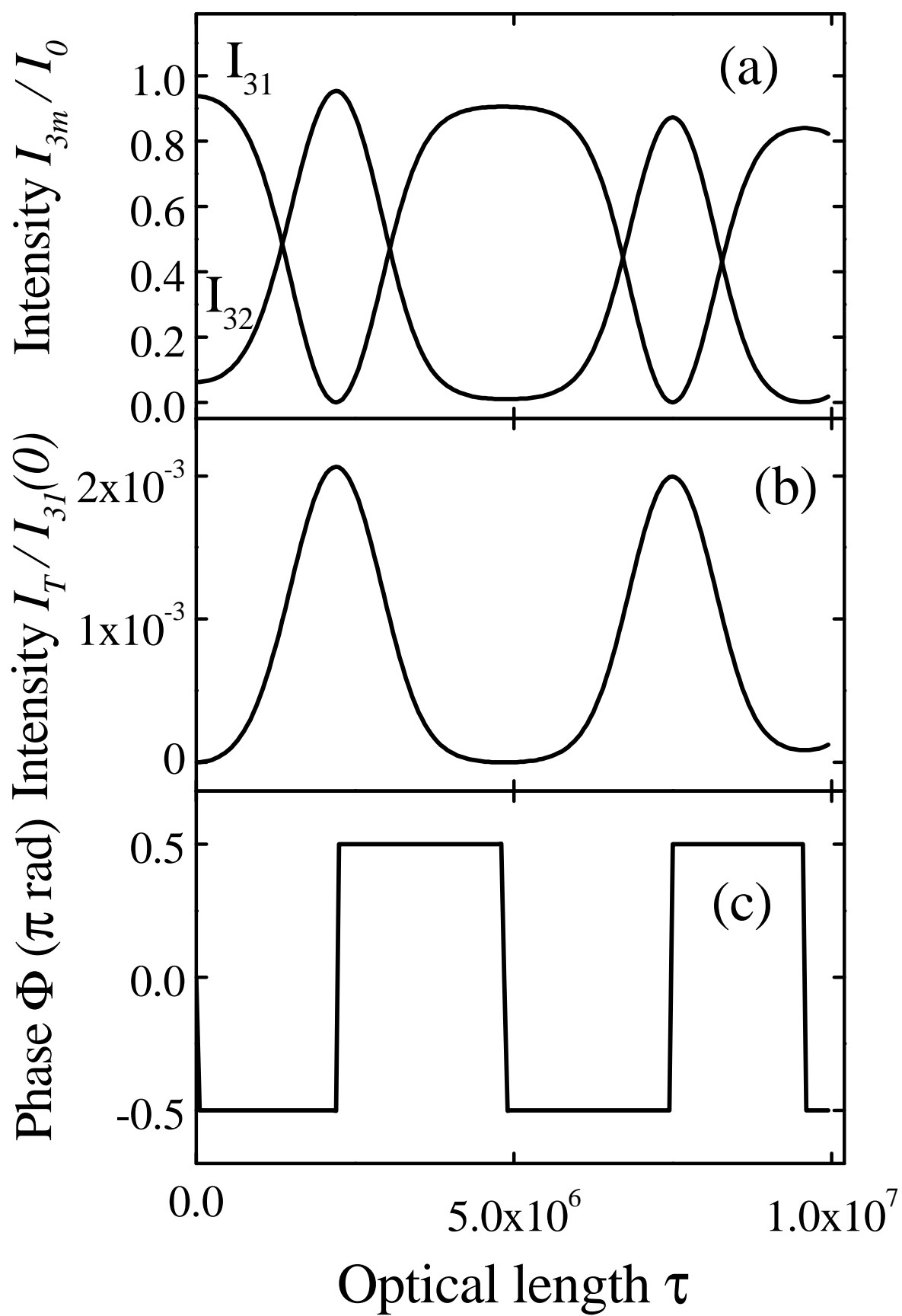


Fig. 3

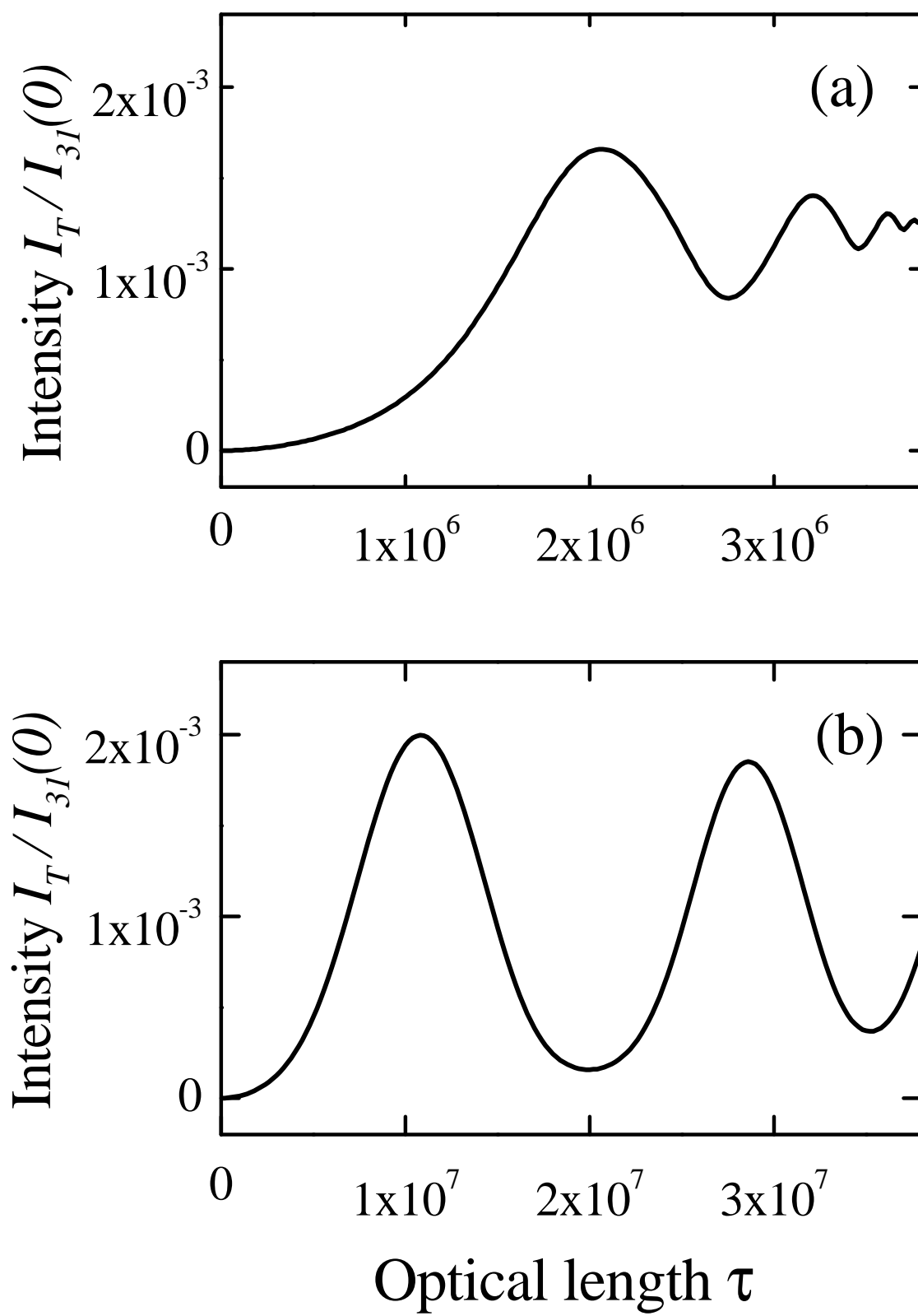


Fig. 4